INFECTION AND IMMUNITY, May 1997, p. 1584–1592 Vol. 65, No. 5
0019-9567/97/$04.00+0

Structure and Biological Activities of Acapsular *Cryptococcus neoformans* 602 Complemented with the *CAP64* Gene

YUN C. CHANG,[1] ROBERT CHERNIAK,[2] THOMAS R. KOZEL,[3] DONALD L. GRANGER,[4] LAURA C. MORRIS,[2] LEANNE C. WEINHOLD,[3] AND K. J. KWON-CHUNG[1]*

Laboratory of Molecular Microbiology, National Institute of Allergy and Infectious Diseases, National Institutes of Health, Bethesda, Maryland 20892[1]; Department of Chemistry, Georgia State University, Atlanta, Georgia 30303[2]; Department of Microbiology, School of Medicine, University of Nevada, Reno, Nevada 89557[3]; and Division of Infectious Diseases, School of Medicine, University of Utah, Salt Lake City, Utah 84132[4]

Received 10 July 1996/Returned for modification 19 September 1996/Accepted 1 February 1997

The extracellular polysaccharide capsule of *Cryptococcus neoformans* is a well-recognized virulence factor. Strain 602 is an acapsular clinical isolate of unknown serotype which has been widely used in studies of virulence and host-parasite interactions. In previous studies, strain 602 was compared with genetically unrelated strains of various serotypes because the wild-type equivalent of strain 602 was not available. We created an encapsulated strain, TYCC38-602, by transforming strain 602 with the *CAP64* gene which was isolated from a serotype D strain. Serological tests and chemical analysis of the major polysaccharide capsule of TYCC38-602 indicated that strain 602 was originally derived from a serotype A strain. Restoration of the ability to produce a capsule enabled strain 602 to cause fatal infection in mice, whereas the acapsular strain 602 remained avirulent. Capsule-restored yeast cells of strain 602 activated the human complement system and bound C3 fragments in a manner that is characteristic of encapsulated cryptococci. In addition, the capsule in TYCC38-602 masked the ability of the organism to induce tumor necrosis factor alpha and subsequent nitric oxide synthase production in primed macrophage-like cells. These results indicate that the lack of capsule in strain 602 is the reason for its inability to cause fatal infection. Moreover, the acapsular phenotype accounts for differences in various biological activities of strain 602 compared to encapsulated strains. The results also indicate that the gene product of *CAP64* does not contribute to serotype specificity of capsules in *C. neoformans*.

Cryptococcus neoformans is an encapsulated yeast which can produce meningoencephalitis, primarily in immunocompromised patients. Capsule formation is a well-recognized virulence factor of *C. neoformans* (reviewed in reference 15). The major capsular polysaccharide, termed glucuronoxylomannan (GXM), consists of an O-acetylated, α-1,3-mannose backbone with xylosyl and glucuronosyl side chains. The extent of O-acetylation and xylosyl substitution varies with serotype. The polysaccharide capsule was originally described as an antiphagocytic surface structure that enabled the fungus to resist destruction by leukocytes (2). As knowledge of this pathogen expanded, additional mechanisms for capsule-related virulence were discovered. The capsule and/or its constituent GXM (i) blocks the potential opsonic effects of anti-cell wall antibodies (25), (ii) masks the signal necessary for tumor necrosis factor alpha (TNF-α) secretion and nitric oxide synthase (NOS) induction in primed macrophages (29), (iii) activates the alternative complement system leading to consumption of complement (24), (iv) interferes with antigen presentation and subsequent T-cell activation for secretion of lymphokines (7, 33), (v) inhibits leukocyte adhesion to endothelium and leukocyte migration into sites of inflammation (8), and (vi) induces suppressor T lymphocytes which down-regulate the cell-mediated immune response (28).

Previous studies on the role of the capsule in virulence and the effect of the capsule on cell-mediated immunity were performed with acapsular mutants of various backgrounds. The most widely used strain for these purposes was the stable acapsular strain 602, originally obtained from a clinical isolate (16). Because the parental strain of this mutant is not available, comparative studies have always been made with strains of various serotypes with unrelated genetic background. Thus, one could not assume that differences observed in the host response between strain 602 and encapsulated strains were solely attributable to the presence of capsule. Due to the lack of a polysaccharide capsule, the serotype of strain 602 could not be determined immunologically, although its DNA fingerprint pattern was most compatible with that of a typical serotype A strain (32). In addition, although the sexual cycle exists in *C. neoformans* (19), mating among strains of serotype A has been of limited use (unpublished observation). This made further characterization of strain 602 difficult. Recent establishment of a transformation system and cloning of capsule-related genes (3, 4, 9) provided the opportunity to characterize the capsular defect of strain 602. In this study, the acapsular phenotype of strain 602 was complemented by a recently cloned *CAP64* gene obtained from a serotype D isolate (4). Thus, the complemented encapsulated isolate could be compared with strain 602 for studies on the role of the polysaccharide capsule as a single variable in host-parasite interactions. This is significant because previous studies of genetically characterized acapsular *C. neoformans* were done with strains of serotype D (3, 4), which is much less frequent cause of cryptococcosis. In this study, we assessed several structural and biological properties of this complemented encapsulated strain 602, including the chemical structure of the capsule polysaccharide, virulence in mice, ability to induce NOS and TNF-α in primed murine macrophage-like cells, and the pattern of interaction with the human complement system.

* Corresponding author. Mailing address: LCI, NIAID, Building 10, Room 11C304, National Institutes of Health, Bethesda, MD 20892. Phone: (301) 496-1602. Fax: (301) 480-0050.

MATERIALS AND METHODS

Strains and genes. Strain 602 is an acapsular strain of unknown serotype originally obtained from a clinical isolate (16). 602FO1 is a spontaneous *ura5* mutant of strain 602 isolated on 5-fluoroorotic acid plates (21). TYCC38-602 is a stable encapsulated strain which was obtained by transforming 602FO1 with pYCC38 which contains the *CAP64* gene (4). CIP3-602 is a stable acapsular strain which was obtained by transforming 602FO1 with a *URA5* vector, pCIP3. B-4500 is a wild-type strain of serotype D generated in our laboratory (20). H99 and 388 are encapsulated clinical isolates of serotype A. The strains ATCC 62066 (serotype A) and ATCC 24065 (serotype B) are the reference strains used for isolation of capsular polysaccharide. B-4130, a Cap64$^-$ strain, was described previously (4). TYCC38-4130 is the same as TYCC38 and was described previously (4). Plasmid pYCC6 contains the *CAP59* gene which was isolated from a serotype D strain, B-3501 (3). Transformation was performed as described previously (9). The Ura5$^+$ transformants were grown on YEPD medium (1% yeast extract, 2% peptone, 2% glucose, 2% agar) to remove selection pressure, and the subsequent Ura5$^-$ cells were tested for the capsular phenotype by India ink staining. Stable Ura5$^+$ transformants were obtained by at least three passages of cells on YEPD medium.

Virulence test. Female BALB/c mice were injected with a 0.2-ml suspension of yeast cells (5×10^5) in the tail vein and monitored for survival. Eight mice were used for each strain.

Serotyping of TYCC38-602. The serotype of TYCC38-602 was determined by dot blot analysis using factor sera provided by Iatron Laboratories (Tokyo, Japan). Strips of nitrocellulose transfer membrane (0.5 by 5 cm) were spotted every centimeter with 1 μl of a freshly prepared solution of GXM and processed as described previously (1).

Production of GXM. TYCC38-602 was grown in 1 liter of a defined glucose broth for 4 days at 37°C as described by Cherniak et al. (5). The culture was autoclaved and centrifuged to remove the cells. Purified GXM was isolated from the culture supernatant fluid by selective precipitation with hexadecyltrimethylammonium bromide as previously described (5). A portion of the purified GXM was dissolved in 10 ml of H_2O and O-deacetylated (GXM-D) by adjusting the pH to 11.25 with NH_4OH and stirring the resulting solution for 24 h at 23°C. Reference GXMs of each serotype were used for comparison.

NMR. ^{1}H nuclear magnetic resonance (NMR) spectra were obtained with a Varian VXR-400 NMR spectrometer equipped with a 5-mm ^{1}H-^{19}F probe and operated at 399.952 MHz for ^{1}H observation. Spectra were recorded at 80°C, and chemical shifts were measured relative to the methyl groups of sodium 4,4-dimethyl-4-silapentane-1-sulfonate taken as 0.00 ppm. Spectra were processed by using the program FELIX (Biosym Technologies, San Diego, Calif.). Each spectrum was resolution enhanced by applying a sine bell window function over all real data points. Spectra of GXMs were compared to spectra of reference GXMs of known chemical structure (6).

Immunofluorescence analysis of C3 binding. Activation and binding of C3 from normal human serum (NHS) to cryptococcal cells was determined as described previously (17). Briefly, formalin-killed cryptococcal cells (6×10^5) were incubated at 37°C with 1.5 ml of 40% NHS in GVB^{2+} (5 mM sodium Veronal-buffered 142 mM saline [pH 7.3] containing 0.1% gelatin, 0.15 mM $CaCl_2$, and 1 mM $MgCl_2$). The serum was a pool prepared from sera obtained from 5 to 10 normal adult donors. Samples were removed after 2, 4, 8, and 16 min, and the cells were washed and stained as described previously (17) with fluorescein-conjugated antiserum to human C3 (Kent Laboratories Inc., Redmond, Wash.). The pattern of C3 binding was determined by fluorescence microscopy using a Bio-Rad MRC-600 confocal imaging system. Images were scanned at 1-μm intervals through the yeast cells and projected onto a single plane.

Kinetics for activation and binding of C3 fragments. The kinetics for activation and binding of C3 fragments to cryptococcal cells were assessed in 1.5-ml reaction mixtures consisting of (i) 40% NHS or 40% heat-inactivated serum, (ii) GVB^{2+}, (iii) ^{125}I-labeled C3 sufficient to provide a specific activity of 45,000 cpm/μg, and (iv) 3×10^6 formalin-killed cryptococcal cells. In some experiments, additional 5 mM Mg^{2+} and 5 mM EGTA (Mg-EGTA) were incorporated into the incubation mixture. The tubes were incubated at 37°C, and 50-μl samples were withdrawn in duplicate at various time intervals between 1 and 50 min. The reaction was stopped by adding each sample to wells of Millipore Multi-Screen-BV filtration plates fitted with 1.2-μm-pore-size Durapore BVPP membranes (Millipore Corporation, Bedford, Mass.) which contained 200 μl of phosphate-buffered saline containing 1% sodium dodecyl sulfate (PBS-SDS) and 20 mM EDTA. The wells were washed four times with PBS-SDS by using the Multiscreen filtration system (Millipore), and the amount of bound radioactivity was determined. Specific binding was determined by subtracting the radioactivity of samples incubated with heat-inactivated serum from the total binding observed with samples incubated with NHS.

Binding data were analyzed as a plot of molecules of bound C3 per cell versus incubation time and as a first-order rate plot in which $\ln(A/A_0)$ is plotted against incubation time (18). A_0 is the total number of possible binding sites and is estimated as the maximum number of C3 molecules bound to each yeast cell during the 50-min incubation period, and A is the number of unoccupied binding sites at a given sample time. Data from the first-order rate plot are summarized as t_0 and k'. t_0 is the lag in initiation before the phase of rapid accumulation of C3 fragments occurs. t_0 is calculated as the time at which $\ln(A/A_0)$ equals zero in the linear portion of a plot of $\ln(A/A_0)$ versus time (see Fig. 5 for examples). k' is the apparent first-order rate constant for the rapid accumulation of C3 that occurs after the lag and is a measure of the rate of accumulation of C3 on each cell type. The derivation and application of the first-order plot to binding of C3 have been described (18).

Macrophage cultures. Macrophage cultures were prepared as described previously (29). To prepare yeast cells for these studies, cryptococcal strains were cultured without agitation for 48 h in yeast nitrogen broth (Gibco) in large flasks (175 cm^2) at 37°C. Early-stationary-phase cells were then washed by centrifugation at $2,000 \times g$ with PBS three times and resuspended at 10^7 cells per ml in PBS. The yeast cells were heat killed at 70°C for 15 min and checked for sterility by plating aliquots on Sabouraud agar. Cryptococci were stored as heat-killed suspensions at 4°C until used. For addition to macrophages, yeast cells were diluted in Dulbecco's modified Eagle's medium (DMEM) and added to cell cultures at various ratios as shown in the figure legends.

A murine macrophage cell line, J774.1 (BALB/c origin), was used to assess inducible NOS (iNOS) activity. Cells were grown at 37°C in 5% CO_2 in DMEM–10% fetal bovine serum (FBS; HyClone Laboratories, Logan, Utah) and passaged every 3 to 4 days in large (105-mm-diameter) non-tissue culture-treated sterile petri plates (Falcon, Lincoln Park, N.J.). DMEM was modified to contain 25 mM glucose, 25 mM sodium bicarbonate, 25 mM morpholine propanesulfonic acid buffer (pH 7.4), 100 Units of penicillin G per ml, and 10 μg of gentamicin per ml.

For experiments, macrophages were rinsed from cell culture plates, washed by centrifugation at $800 \times g$ at 4°C, and plated in 16-mm-diameter wells (Costar, Cambridge, Mass.) at 500,000 cells per chamber in 1.0 ml of medium. Recombinant murine gamma interferon (IFN-γ; kindly provided as a gift from Genentech, South San Francisco, Calif.) was added to each experimental well at a concentration of 200 U/ml. After overnight incubation, fresh medium was added along with heat-killed yeast cells. Endotoxin (*Escherichia coli* 128:B12; Sigma Chemical Co., St. Louis, Mo.) was added to positive control wells at 1.0 μg/ml. The cultures were incubated for approximately 40 h; supernatant fluids were removed, microcentrifuged to remove cells, and stored frozen until assayed.

Assay for macrophage iNOS. Aliquots (50 μl) of macrophage supernatant fluids were mixed with 200 μl of Greiss reagent (11) in microtiter wells. The resulting colorimetric reaction was measured at 570 nm in a microplate reader (Dynatech MR700), and the concentrations of the experimental samples were calculated from a linear curve constructed with sodium nitrite standards (0 to 150 μM). The data were calculated as micromoles of nitrite produced per 5×10^5 cells per 40 h. Results are expressed as the percentage of the maximal response for a particular experiment. The maximal response is defined as the amount of nitrite produced per 40 h in the positive control cultures containing IFN-γ plus endotoxin. In no instance did any of the experimental conditions result in nitrite production which exceeded that of the positive control. In no instance did untreated J774.1 cells produce nitrite. All experimental conditions were run in duplicate or triplicate.

Assay for TNF-α. Supernatant fluids from macrophages challenged with heat-killed yeasts were stored frozen (−80°C) until assayed. L929 continuous fibroblast cells were counted, plated at 25,000 cells per microtiter well in 0.1 ml of DMEM–10% FBS, and preincubated for 24 h at 37°C in 5% CO_2. TNF-α supernatant fluids (100 μl) were diluted in DMEM–10% FBS containing 3.0 μg of actinomycin D per ml and were added to L929 cells after removal of the preincubation medium. The cultures were then incubated under the same conditions for 16 to 20 h to allow for TNF-induced killing. The remaining living cells were detected by adding MTT (2.5 mg/ml in PBS), 20 μl/well, and incubating the plates for 2.5 h. Then the plates were centrifuged for 10 min at $500 \times g$, and the supernatant fluids were removed and discarded. The remaining insoluble MTT crystals were dissolved for 1 h in dimethylformamide containing 20% SDS. Soluble reduced MTT was quantitated in a microplate reader at 570 nm. TNF-α concentration in supernatant fluids was calculated from a standard curve constructed with known concentrations (in units/milliliter) of recombinant murine TNF-α (0.01 to 1,000 U/ml). One unit is defined as the amount of TNF-α giving 50% lysis of actinomycin D-treated L929 cells under the above-specified conditions. The endpoints of L929 cell lysis/no lysis were determined by comparison with 10% SDS-lysed L929 cells and untreated control (no TNF-α) cells, respectively. Units of TNF-α per milliliter were calculated according to the formula in reference 26. The data were expressed as geometric mean titers of twofold dilution series (beginning with a 1/2 dilution) run in duplicate or triplicate per supernatant. All supernatant fluids were assayed at least twice.

RESULTS

***CAP64* complements the acapsular phenotype of strain 602.** Cells of strain 602FO1 transformed with plasmid pYCC38 containing *CAP64* produced capsules, while those transformed with vector alone (pCIP3) or with plasmid pYCC6 containing *CAP59* remained acapsular. The encapsulated transformants became acapsular when cells lost plasmid pYCC38 as determined by loss of the *URA5* marker (see Materials and Meth-

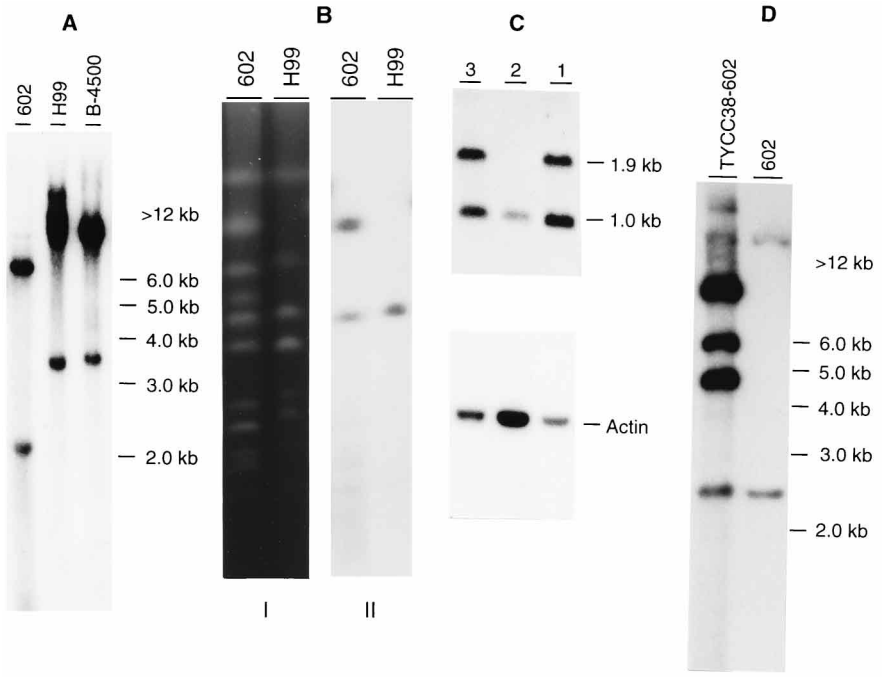

FIG. 1. Structure and expression of *CAP64*. (A) Southern blot analysis. DNA isolated from strain 602 and two wild-type strains (B-4500 and H99) was digested with *Pst*I and separated on 0.8% agarose gel. The blot was hybridized with a probe of pYCC38. (B) CHEF analysis. To determine the chromosomal location of *CAP64* in strain 602 and H99, chromosomes were isolated, separated, and stained with ethidium bromide as described previously (2) (I). The blot was hybridized with a probe of pYCC38 (II). (C) Northern blot analysis. PolyA$^+$ RNAs were isolated and separated on formaldehyde-agarose gel. The blot was hybridized with a probe of pYCC38. Lane 1, B-4130 (Cap64$^-$); lane 2, 602; lane 3, Cap64$^+$ strain. The 1.9- and 1.0-kb signals represent *CAP64* and *PRE1* transcripts, respectively. The same blot was stripped and hybridized with an actin gene probe to show similar loading of RNA. (D) Southern blot analysis. DNA isolated from strains 602 and TYCC38-602 was digested with *Xba*I and separated on an 0.8% agarose gel. The blot was hybridized with a probe of pYCC38.

ods). These results suggested that the defect of strain 602 is *CAP64* related. The genomic structure of *CAP64* in strain 602 is different from that in standard reference strains as shown by Southern and contour-clamped homogeneous electric field (CHEF) blotting (Fig. 1A and B). This finding was further supported by using *CAP64* cDNA as a probe (data not shown). The signals on two different chromosomes in the CHEF blot suggested that strain 602 may contain a translocation or two copies of a *CAP64*-like sequence. Although the presence of *CAP64* DNA in strain 602 was evident, *CAP64* transcript was absent in strain 602 by Northern analysis (Fig. 1C). One of the stable encapsulated transformants, TYCC38-602, was chosen for further study. Southern analysis of TYCC38-602 suggested that it contains ectopic insertions of plasmid pYCC38 (Fig. 1D).

We tested the virulence of the encapsulated TYCC38-602 in mice. All mice infected with TYCC38-602 died within 25 days (Fig. 2A), while those injected with CIP3-602 remained healthy for 6 months. The brain smear prepared from one of the TYCC38-602-infected mice which died on day 25 showed numerous encapsulated yeast cells (Fig. 2B). One of the mice injected with CIP3-602 was sacrificed at the end of 6 months, and the brain was removed for culture. Only two colonies of *C. neoformans* from the brain grew, and these yeast cells contained no capsule (not shown). These results suggested that the avirulence of strain 602 was due to a defect in the *CAP64* gene.

Chemical structure of the GXM from TYCC38-602. The serotype of TYCC38-602 was first determined by dot blot analysis with factor sera. This result showed that complemented strain 602 reacts with antisera specific for factors 1, 2, 3, and 7, a pattern consistent with serotype A. We further determined the chemical structure of the major polysaccharide from TYCC38-602. The NMR analytical data indicated that insertion of *CAP64* in the genome of strain 602 resulted in the synthesis of a typical serotype A polysaccharide (Fig. 3A). A minor portion of the GXM contained serotype B structure as well, although this was not reflected in the dot blot analysis with factor sera. When the same gene was transformed into an acapsular mutant (*cap64*) of serotype D, B-4130, it complemented the acapsular phenotype (4) and produced a polysaccharide pattern typical of serotype D. We also noted that TYCC38-4130 produced a minor polysaccharide of no defined serotype (Fig. 3B). Dot blot analysis of TYCC38-4130 demonstrated reaction with antisera specific for factors 1, 2, 3, and 8, a typical serotype D pattern, although the reactions were not as intense as those generated by a wild-type GXM.

Activation and binding of C3 fragments by TYCC38-602. Previous studies found that incubation of nonencapsulated cryptococci in NHS leads to binding of antiglucan antibodies to the cell wall, initiation of the classical complement system, and deposition of C3 fragments onto the cell wall (14, 17, 34). This pattern of C3 binding is characterized by early and synchronous deposition of C3 over the entire surface of the yeast cells. In contrast, encapsulated cryptococci do not bind the antiglucan antibody found in NHS and initiate the complement system only via the alternative complement pathway. Activation and binding of C3 to encapsulated cryptococci is characterized by a slow, asynchronous formation of focal sites of C3 deposition that are amplified with additional incubation time to cover the cryptococcal capsule.

An experiment was done to assess the manner in which the transformed cryptococcal strain interacted with the human complement system. The site of C3 binding was determined after incubation for various time intervals with NHS. Incuba-

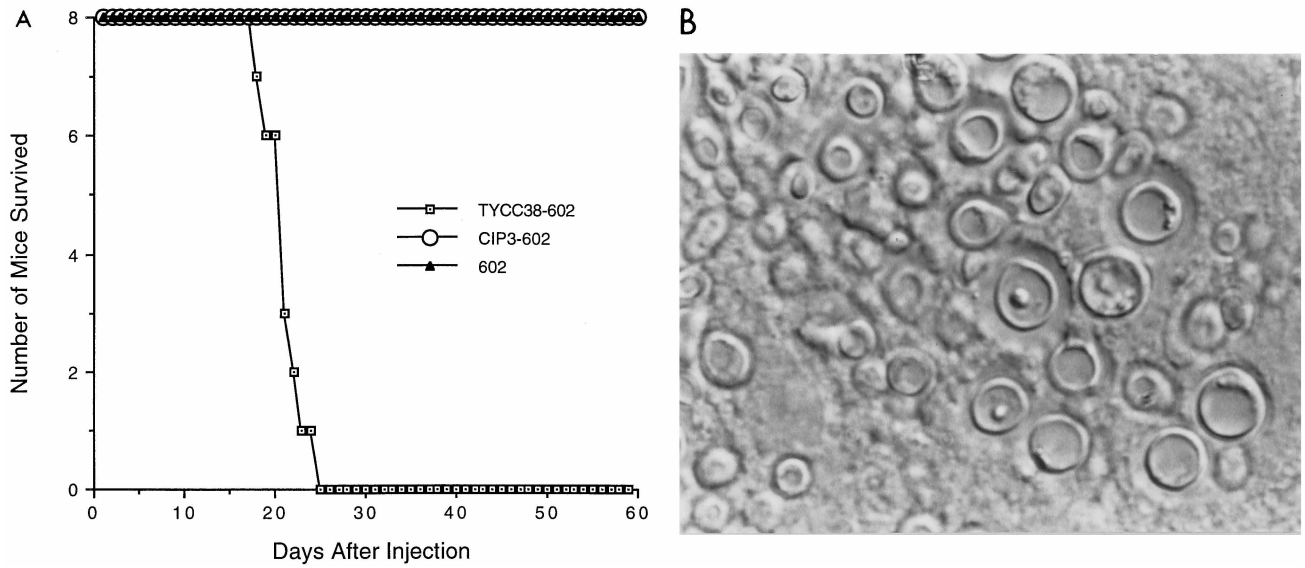

FIG. 2. (A) Virulence test. Groups of eight mice each were injected with 5×10^5 viable cells and monitored to determine survival. (B) Brain smear showing the cells of TYCC38-602. Brain tissue of a mouse infected by TYCC38-602 which died on day 25 was smeared on a slide and observed by light microscopy (magnification, ×1,200).

tion of cells of strain 602 in serum led to immediate binding of C3 over the entire surface of the yeast (Fig. 4). This was readily apparent after 2 min. Additional incubation led to an increase in the density of bound C3, as shown by an increase in the intensity of fluorescence staining. Incubation of the encapsulated strain 388 in serum was characterized by a very slow initial accumulation of C3. No bound C3 was apparent after 2 min. After 4 min of incubation, focal deposits of bound C3 were observed at random sites which appeared to expand with continued incubation to fill the capsule. The pattern for activation and binding of C3 to TYCC38-602 was similar to that observed with the encapsulated strain 388.

An experiment was done to characterize the kinetics for accumulation of C3 fragments on the transformant TYCC38-602. Experiments were done in the presence and absence of Mg-EGTA to evaluate the role of the classical complement pathway in early kinetics. Treatment of serum with Mg-EGTA chelates the calcium needed for activation of the classical pathway while leaving Mg^{2+} available for activation of the alternative pathway (10, 30). The kinetics for activation and binding of C3 to encapsulated strain 388 showed that there was a substantial lag before the phase of rapid accumulation of C3 on the yeast cells (t_0 = 9.0 min [Fig. 5]). This was followed by a rapid accumulation of C3 (k' = 0.20) and an abrupt termination of binding after approximately 15 to 20 min. Incorporation of Mg-EGTA into the incubation medium slightly reduced the lag (t_0 = 7.1 min) and had no effect on the rate of C3 binding during the rapid accumulation phase (k' = 0.20).

Incubation of nonencapsulated strain 602 in normal human serum led to an early accumulation of C3 on the yeast cells (t_0 = 3.6 min) followed by a more gradual phase of rapid accumulation (k' = 0.17) than was observed with encapsulated strain 388. Treatment of serum with Mg-EGTA introduced a substantial lag before the period of rapid accumulation of C3 fragments on strain 602 (t_0 = 18 min), indicating a significant role for the classical pathway in early activation kinetics.

The kinetics for activation and binding of C3 to the transformed TYCC38-602 resembled several aspects of the kinetics observed with encapsulated strain 388. First, there was a lag of approximately 4.7 min before the rapid accumulation phase, although the lag was not as long as that seen with strain 388. Second, the first-order rate constant (k' = 0.21) indicated rapid accumulation of C3 once past the lag phase. Third, there was an abrupt and early termination of the rapid accumulation phase after approximately 10 to 15 min. Finally, similar to results observed with encapsulated strain 388, treatment of serum with Mg-EGTA slightly reduced the length of the lag phase (t_0 = 3.9 min) and had no effect on the first-order rate constant (k' = 0.21), indicating that initiation occurs solely via the alternative pathway.

Capsule acquisition leads to loss of induction of TNF-α and NOS in murine macrophages. It was reported previously that unlike other species of fungi, *C. neoformans* did not induce NOS expression in IFN-γ-primed macrophages (29). However, when seven different acapsular mutant strains of *C. neoformans*, including strain 602, were used to challenge primed macrophages, iNOS expression occurred (29). Two wild-type parent strains of three of the acapsular mutant strains failed to induce NOS in macrophages. Therefore, it seemed likely that the capsule-positive phenotype of *C. neoformans* was responsible for the lack of induction of this host defense enzyme activity in macrophages. But because the acapsular strains were derived by chemical mutagenesis, the lack of NOS induction in primed macrophages may have been due to other unknown mutations.

Complementation of the acapsular mutant strain 602 with the *CAP64* gene allowed for a definitive experiment to test whether the capsule-positive phenotype was responsible for lack of induction of NOS in primed macrophages. All *C. neoformans* strains were grown to early stationary phase in YNB liquid medium, washed by centrifugation in PBS, and heat killed. Monolayers of J774.1 macrophage-like cells were primed overnight with IFN-γ and then challenged with known numbers of the yeast strains. After a 40-h incubation, supernatant fluids from macrophage cultures were assayed for nitrite, an end product of the NOS-catalyzed oxidation of arginine guanidino nitrogen to nitric oxide (13). The results of five separate experiments measuring iNOS activity are normalized

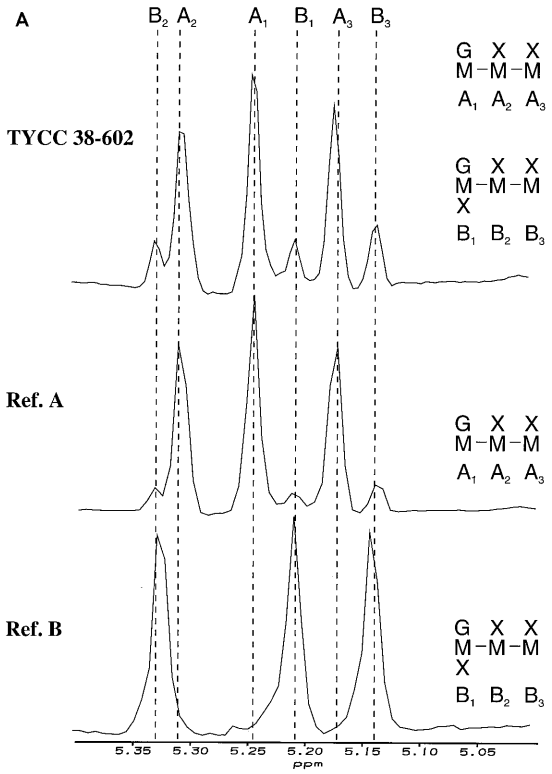

B **TYCC38-4130**

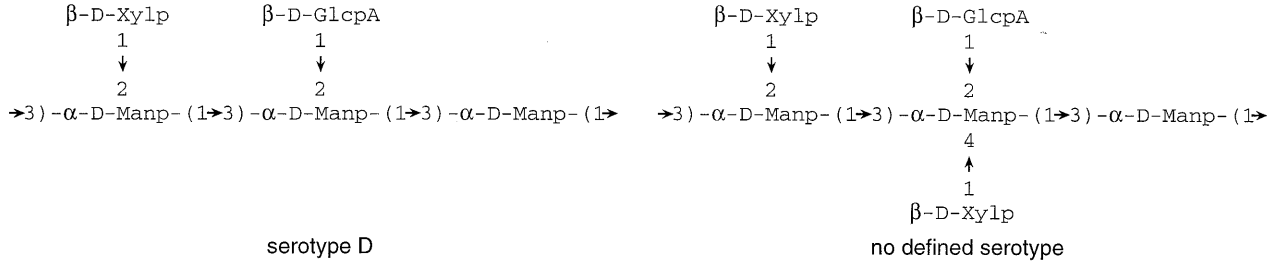

TYCC38-602

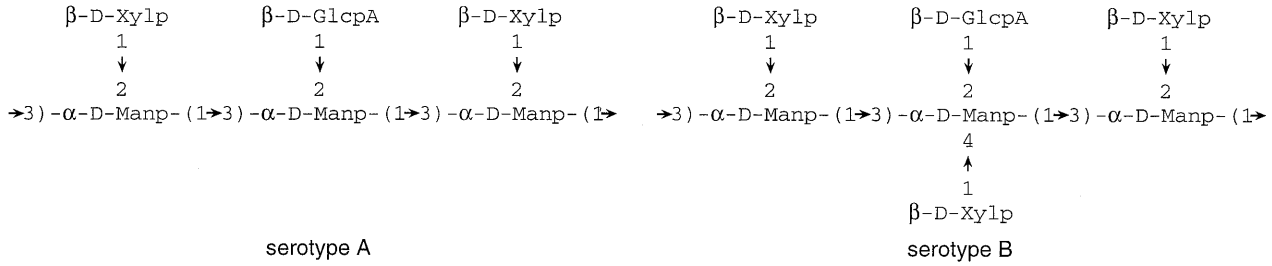

FIG. 3. Chemical structure of GXM. (A) Resolution-enhanced mannose anomeric region of the ^{1}H NMR spectra of the GXM from TYCC38-602, reference serotype A isolate ATCC 62066 (Ref. A), and reference serotype B isolate ATCC 24065 (Ref. B). The mannose residues of each O-deacetylated GXM have been labeled with the corresponding triad elements presented to the right of each spectrum. (B) The GXM chemical structures of TYCC38-4130 and TYCC38-602.

as percentages of the maximal response (Fig. 6A). Maximal response is defined as micromoles of nitrite produced per 500,000 macrophages per 40 h upon activation with IFN-γ and endotoxin. This treatment protocol consistently gives the highest activity of iNOS in these macrophages (31). The acapsular strains 602 and CIP3-602 resulted in NOS induction in IFN-γ-primed macrophages at all yeast/macrophage ratios tested from 1:100 to 10:1. At the optimal ratios for induction (1:2 to

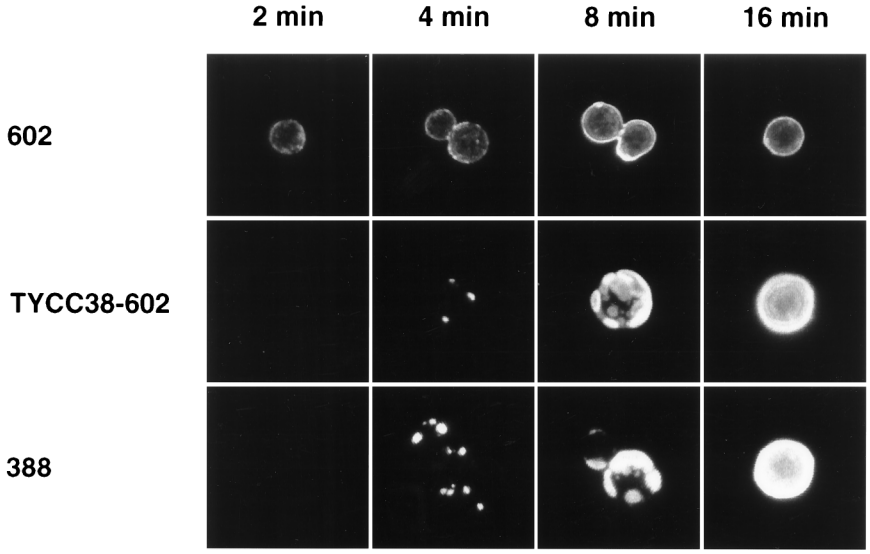

FIG. 4. Sites for deposition of C3 fragments on strain 602, strain TYCC38-602, and encapsulated clinical strain 388 incubated in 40% NHS for 2, 4, 8, or 16 min. Sites of C3 deposition were identified by use of fluorescein-labeled antiserum to C3 and examination by confocal microscopy.

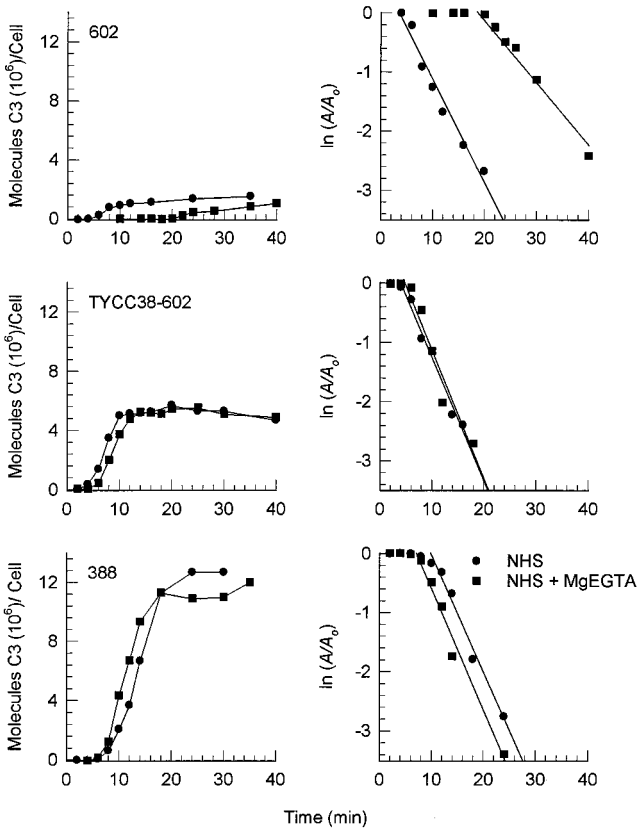

FIG. 5. Analysis of the kinetics for activation and binding of C3 fragments to strain 602, strain TYCC38-602, and encapsulated clinical strain 388. The panels on the right depict a kinetic analysis of the consumption of available sites for C3 binding to the yeast cells, where A_0 is the maximum number of apparent sites available for C3 binding and A is the number of unoccupied sites at each time interval (see text).

5:1), the acapsular strains induced 60 to 80% of the maximal response. In raw numbers, this is approximately 70 μmol of nitrite per 5×10^5 cells per 40 h. In Fig. 6A, 0% is set to the amount of nitrite produced by untreated macrophages not challenged with cryptococci, which was always produced undetectable levels of nitrite (less than 5 μmol per 5×10^5 macrophages per 40 h). Unchallenged IFN-γ-primed macrophages consistently produced low levels of nitrite (Fig. 6; these controls are illustrated at each of the yeast/macrophage ratios tested). The encapsulated TYCC38-602 strain did not induce NOS in primed macrophages unless the yeast/macrophage ratio was raised to 3:1 to 10:1 (Fig. 6). At the highest ratio tested (10:1), iNOS activity was only about 30% of the maximal response. Thus, the acapsular strains induced NOS activity at 100-fold fewer yeasts per macrophage compared to the encapsulated strain. Not shown are controls for iNOS activity of macrophages lacking treatment with IFN-γ and challenged with the strains of cryptococci at the various ratios shown in Fig. 6. Under these conditions, iNOS activity was never seen. These results point to the capsule-positive phenotype as the critical factor for NOS induction by *C. neoformans*. The results further suggest that one aspect of the virulence potential mediated by the capsule is to mask the fungi from a macrophage recognition step which results in iNOS gene transcription and ultimately the production of growth-inhibitory nitric oxide by mononuclear phagocytes (12).

Because induction of iNOS in IFN-γ-primed macrophages is mediated via an autocrine loop where the microorganism induces macrophage TNF-α secretion, and TNF-α feeds back on the macrophage through receptor binding and initiation of iNOS gene transcription, we questioned whether TNF-α assays for the different strains would correlate with the iNOS activity results. TYCC38-602 and the acapsular control strains (602 and CIP3-602) were added to IFN-γ-primed J774.1 cells at different yeast/macrophage ratios. Supernatant fluids were collected after 40 h of incubation and assayed for TNF-α concentrations, using a standard bioassay method (26, 27). Over a wide range of yeast/macrophage ratios, encapsulated strain TYCC38-602 failed to trigger TNF-α secretion by macrophages (Fig. 6B). In contrast with the acapsular strains, TNF-α

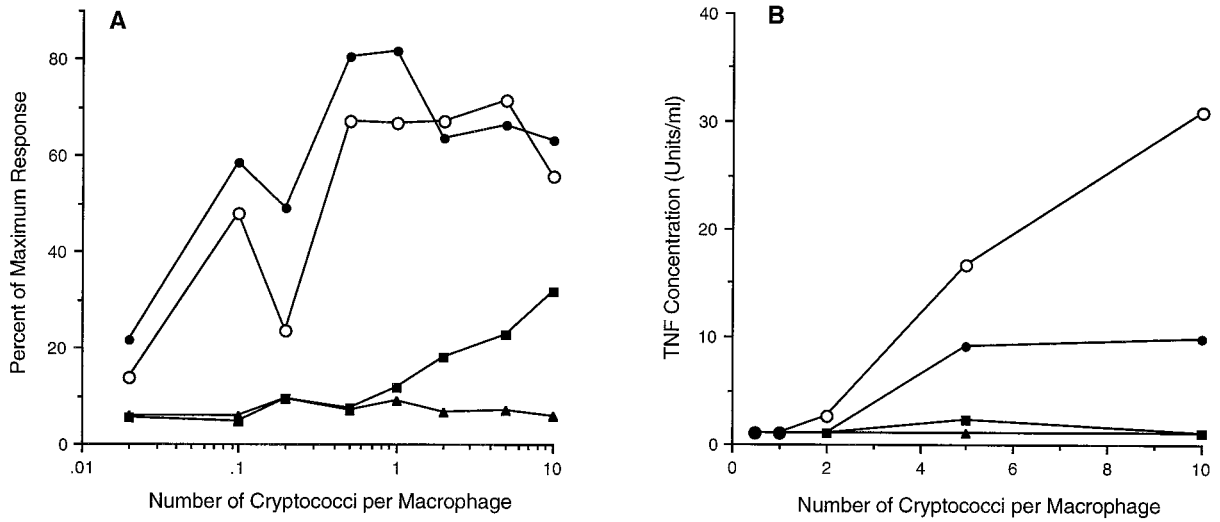

FIG. 6. TNF-α secretion and iNOS activity in IFN-γ-primed J774.1 macrophages challenged with strains of *C. neoformans* which are capable or incapable of capsule formation. (A) iNOS activity as a percentage of the maximal response (defined as the activity for IFN-γ-primed J774.1 cells treated with 1.0 μg of endotoxin per ml) for macrophages challenged with strains 602 (open circles), CIP3-602 (closed circles), and TYCC38-602 (squares) at the yeast/macrophage ratios shown. The triangles show the activity of the control macrophages treated with IFN-γ (200 U/ml) alone. Values are the means of the combined results of five separate experiments. At yeast/macrophage ratios of less than 0.5:1, points are from single experiments. At ratios equal to or greater than 0.5:1, values are the means from two to three experiments. (B) TNF-α concentrations in supernatant fluids from macrophage-cryptococcus cocultures at the yeast/macrophage ratios shown. The symbols represent the strains as designated above. The values are the means from five separate experiments.

secretion was induced at yeast/macrophage ratios of 5:1 to 10:1. The CIP3-602 strain was consistently more active for TNF-α induction than strain 602. It is not entirely clear why this was the case. Perhaps ectopic integration of pCIP3 alters the fungal cells in some way which changes recognition by macrophages. By comparison, the two assays (iNOS and TNF-α) correlated with respect to the encapsulated and acapsular strains. Capsule presence masks the organism from TNF-α induction and subsequent iNOS expression by macrophages. However, this difference is detected at far lower fungal cell numbers (relative to constant macrophage number) by iNOS assay compared to TNF-α assay. The most likely explanation is the degree of sensitivity of the two assays. The TNF-α bioassay may be much less sensitive for detecting organism-induced signaling in the macrophage. Alternatively, iNOS induction may occur via a TNF-α circuit operating intracellularly or at the cell surface under conditions where the extracellular fluid-phase TNF-α concentration is at a subdetectable level. Another possibility is that NOS induction occurs via a TNF-independent pathway. Neutralization experiments using a monoclonal antibody against TNF-α may help resolve this question. A more sensitive TNF-α assay using enzyme-linked immunosorbent assay methodology may also provide illuminating results.

DISCUSSION

C. neoformans 602 has been widely used for studies of the role of the polysaccharide capsule in virulence and host defense mechanisms. However, the lack of a suitable isogenic strain of 602 limited the ability to draw solid conclusions regarding the biological activities of the acapsular phenotype. We created an encapsulated strain by ectopic integration of the *CAP64* gene in strain 602. Gene replacement of *CAP64* by homologous integration in strain 602 would make an ideal strain for our studies. However, it is difficult to construct such a strain due to the low frequency of homologous integration. Construction of an ideal 602-derived encapsulated strain by classical recombination is also hampered by the lack of a serotype A strain that can mate with strain 602. Restoration of capsule formation in strain 602 suggested that the acapsular phenotype of strain 602 was due to defects associated with *CAP64*. Serological testing of the complemented strain, TYCC38-602, indicated that strain 602 originated from a serotype A strain. This confirmed our previous conclusion based on the DNA fingerprint pattern analyzed with the probe UT4-P (32). Since the *CAP64* gene from a serotype D isolate complemented the acapsular phenotype of a serotype A strain, the gene product of *CAP64* does not appear to contribute directly to the serotypic specificity of *C. neoformans* polysaccharide capsule.

Chemical structures of the capsular polysaccharide produced in the encapsulated strain, TYCC38-602, were comprised of triads typical of serotype A (Fig. 3). Additional triads similar to those of serotype B were detected as minor components. Minor components were also detected in the serotype D polysaccharide produced in TYCC38-4130, which was originally an acapsular serotype D mutant complemented with *CAP64* (data not shown). We detected such minor components even in the polysaccharide produced by wild-type strain B-3501 (serotype D) when it was transformed with vector (pCIP3) alone (data not shown). These results indicate that the minor components were not due to introduction of *CAP64* but could have resulted from the effects of electroporation or physiological or genetic changes caused by the transformation.

Transformation of nonencapsulated strain 602 to restore capsule formation produced yeast cells which activated and bound C3 fragments in a manner that is characteristic of encapsulated cryptococci. The pattern of early deposition was focal, indicating relatively slow formation of activation nuclei. Previous studies have shown that this asynchronous production of focal initiation sites is due to activation of the alternative complement pathway, with no involvement of the classical pathway (17). This interpretation of the results is supported by kinetic studies (Fig. 5) which found that treatment of serum with Mg-EGTA did not introduce a delay into the kinetics for

activation and binding of C3 to either encapsulated strain 388 or the capsule-restored TYCC38-602. The lag observed before rapid accumulation of C3 fragments on TYCC38-602 was longer than the lag observed with nonencapsulated strain 602 but was somewhat shorter than the lag found with encapsulated strain 388. The factors that influence the length of the lag before rapid amplification on encapsulated cryptococci are not known (35).

Transformation of strain 602 to capsule formation greatly increased the amount of C3 bound to each yeast cell. Presumably this reflects the increased number of binding sites provided by the three-dimensional capsular matrix compared to the two-dimensional surface of cells lacking a capsule. The maximum number of C3 fragments bound to TYCC38-602 was less than the number of C3 fragments bound to encapsulated strain 388. Strain 388 has a capsule that is somewhat larger than the capsule of TYCC38-602. Previous studies have found that large capsule size is associated with increased binding of C3 fragments (35).

Studies of complement activation by nonencapsulated strain 602 showed involvement of the classical pathway in early initiation events. Early binding of C3 appeared as a diffuse, synchronous pattern of binding that previous studies have shown to be due to initiation of the classical pathway via an antiglucan immunoglobulin G antibody that is found in all human sera examined to date (14, 18). The delay in initial activation kinetics with TYCC38-602 suggests that transformation of strain 602 to capsule formation blocks the epitopes that would be recognized by this antibody such that activation of the classical pathway is impossible. This implies that the molecular organizations at the interface between the capsule and the cell wall found with strain TYCC38-602 and encapsulated strains of *C. neoformans* are similar with regard to the ability to block binding of anti-cell wall antibody.

It is well established that once macrophages have become activated by exposure to lymphokines, primarily IFN-γ, their cytotoxic activity is not expressed until they physically engage the invading microorganism itself. Interaction of the primed macrophage (defined as a macrophage with previous or concurrent exposure to activating cytokines, i.e., IFN-γ) with a microorganism results in synergism for cytotoxic functions, especially nitric oxide-mediated cytotoxicity (22). Often the synergistic effect is mediated through TNF-α secretion by the macrophage, which feeds back via an autocrine loop to induce expression of iNOS and other cytotoxic functions. At the molecular level, this mechanism involves enhanced transcription of the iNOS gene in the presence of two signals (i.e., IFN-γ and TNF-α), with little or no transcriptional activation provided by either signal alone (23). The result is the synthesis of a large enzyme (iNOS) activity within the macrophage cytosol leading to production of high-level nitric oxide output. Nitric oxide production at this high level is capable of blocking fungal cell replication and possibly killing fungal cells.

The data shown here point to the capsule as a virulence factor which masks recognition of fungal cells by primed macrophages. Nitric oxide production was detected only under conditions where encapsulated cryptococci (TYCC38-602) outnumbered macrophages by 2 to 1. By contrast, iNOS expression induced by acapsular strains was present at 2 yeast cells per 100 macrophages. The TNF-α secretion response by macrophages paralleled the iNOS results with respect to the encapsulated and acapsular strains. It is possible that yeast cell wall components such as mannans are recognized by macrophages for the induction of proinflammatory cytokine secretion and that when capsular polysaccharide is covering these components, recognition of yeast cells is blocked. The outcome would be failure of a fungistatic mechanism allowing for continued replication of cryptococci in many tissues of the host until the organism burden ascended to the threshold for cytokine induction in macrophages. One potential caveat in this analysis is that the mutation in strain 602 could occupy a proximal step in the pathway of capsule synthesis, possibly affecting the cell wall, rather than a more downstream event involving construction of the capsule itself. If this is the case, then it is conceivable that the difference in biologic activity between strains 602 and TYCC38-602 is due to a difference in cell wall structure, not presence or absence of capsule. Although this seems an unlikely possibility, it nevertheless cannot be excluded at present. Once a better understanding of the pathway of capsule synthesis is achieved, construction of a series of mutants at proximal and distal stages in this process will provide the appropriate tools to resolve this question.

Our studies provide conclusive evidence that (i) *CAP64* from serotype D complements the defect of capsular formation in strain 602; (ii) the acapsular phenotype of strain 602 is a major contributing factor for its behavioral differences compared to that of the encapsulated strains; (iii) the capsule is responsible for the characteristic complement activating properties of encapsulated cryptococci; and (iv) capsule prohibits the induction of NOS as well as TNF-α secretion by INF-γ-primed macrophages.

ACKNOWLEDGMENTS

This work was supported in part by U.S. Public Health Service grants AI 14209 (T.R.K.) and 31769 (R.C.).

REFERENCES

1. **Belay, T., and R. Cherniak.** 1995. Determination of antigen binding specificities of *Cryptococcus neoformans* factor sera by enzyme-linked immunosorbent assay. Infect. Immun. **63:**1810–1819.
2. **Bulmer, G. S., and M. D. Sans.** 1967. *Cryptococcus neoformans*. II. Phagocytosis by human leukocytes. J. Bacteriol. **94:**1480–1483.
3. **Chang, Y. C., and K. J. Kwon-Chung.** 1994. Complementation of a capsule-deficient mutation of *Cryptococcus neoformans* restores its virulence. Mol. Cell. Biol. **14:**4912–4919.
4. **Chang, Y. C., L. A. Penoyer, and K. J. Kwon-Chung.** 1996. The second capsule gene of *Cryptococcus neoformans*, *CAP64*, is essential for virulence. Infect. Immun. **64:**1977–1983.
5. **Cherniak, R., L. C. Morris, B. C. Anderson, and S. A. Meyer.** 1991. Facilitated isolation, purification, and analysis of glucuronoxylomannan of *Cryptococcus neoformans*. Infect. Immun. **59:**59–64.
6. **Cherniak, R., L. C. Morris, T. Belay, E. D. Spitzer, and A. Casadevall.** 1995. Variation in the structure of glucuronoxylomannan in isolates from patients with recurrent cryptococcal meningitis. Infect. Immun. **63:**1899–1905.
7. **Collins, H. L., and G. J. Bancroft.** 1991. Encapsulation of *Cryptococcus neoformans* impairs antigen-specific T-cell responses. Infect. Immun. **59:** 3883–3888.
8. **Dong, Z. M., and J. W. Murphy.** 1995. Intravascular cryptococcal culture filtrate (CneF) and its major component, glucuronoxylomannan, are potent inhibitors of leukocyte accumulation. Infect. Immun. **63:**770–778.
9. **Edman, J. C., and K. J. Kwon-Chung.** 1990. Isolation of the *URA5* gene from *Cryptococcus neoformans* var. *neoformans* and its use as a selective marker for transformation. Mol. Cell. Biol. **10:**4538–4544.
10. **Fine, D. P., S. R. Marney, Jr., D. G. Colley, J. S. Sergent, and R. M. Des Prez.** 1972. C3 shunt activation in human serum chelated with EGTA. J. Immunol. **109:**807–809.
11. **Green, L. C., D. A. Wagner, J. Glogowski, P. L. Skipper, J. S. Wishnok, and S. R. Tannenbaum.** 1982. Analysis of nitrate, nitrite, and [15N]nitrate in biological fluids. Anal. Biochem. **126:**131–138.
12. **Green, S. J., R. M. Crawford, J. T. Hockmeyer, M. S. Meltzer, and C. A. Nacy.** 1990. *Leishmania* major amastigotes initiate the L-arginine-dependent killing mechanism in IFN-gamma-stimulated macrophages by induction of tumor necrosis factor-alpha. J. Immunol. **145:**4290–4297.
13. **Hibbs, J. B., Jr., R. R. Taintor, and Z. Vavrin.** 1987. Macrophage cytotoxicity: role for L-arginine deiminase and imino nitrogen oxidation to nitrite. Science **235:**473–476.
14. **Keller, R. G., G. S. Pfrommer, and T. R. Kozel.** 1994. Occurrences, specificities, and functions of ubiquitous antibodies in human serum that are reactive with the *Cryptococcus neoformans* cell wall. Infect. Immun. **62:**215–220.

15. **Kozel, T. R.** 1995. Virulence factors of *Cryptococcus neoformans*. Trends Microbiol. **3:**295–299.
16. **Kozel, T. R., and J. J. Cazin.** 1971. Non-encapsulated variant of *Cryptococcus neoformans*. I. Virulence studies and characterization of soluble polysaccharide. Infect. Immun. **3:**287–294.
17. **Kozel, T. R., M. A. Wilson, and J. W. Murphy.** 1991. Early events in initiation of alternative complement pathway activation by the capsule of *Cryptococcus neoformans*. Infect. Immun. **59:**3101–3110.
18. **Kozel, T. R., M. A. Wilson, and W. H. Welch.** 1992. Kinetic analysis of the amplification phase for activation and binding of C3 to encapsulated and nonencapsulated *Cryptococcus neoformans*. Infect. Immun. **60:**3122–3127.
19. **Kwon-Chung, K. J.** 1975. A new genus, Filobasidiella, the perfect state of *Cryptococcus neoformans*. Mycologia **67:**1197–2000.
20. **Kwon-Chung, K. J., J. C. Edman, and B. L. Wickes.** 1992. Genetic association of mating types and virulence in *Cryptococcus neoformans*. Infect. Immun. **60:**602–605.
21. **Kwon-Chung, K. J., A. Varma, J. C. Edman, and J. E. Bennett.** 1992. Selection of *ura5* and *ura3* mutants from the two varieties of *Cryptococcus neoformans* on 5-fluoroorotic acid medium. J. Med. Vet. Mycol. **30:**61–69.
22. **Liew, F. Y., Y. Li, and S. Millott.** 1990. Tumor necrosis factor-alpha synergizes with IFN-gamma in mediating killing of *Leishmania* major through the induction of nitric oxide. J. Immunol. **145:**4306–4310.
23. **Lorsbach, R. B., and S. W. Russell.** 1992. A specific sequence of stimulation is required to induce synthesis of the antimicrobial molecule nitric oxide by mouse macrophages. Infect. Immun. **60:**2133–2135.
24. **Macher, A. M., J. E. Bennett, J. E. Gadek, and M. M. Frank.** 1978. Complement depletion in cryptococcal sepsis. J. Immunol. **120:**1686–1690.
25. **McGaw, T. G., and T. R. Kozel.** 1979. Opsonization of *Cryptococcus neoformans* by human immunoglobulin G: masking of immunoglobulin G by cryptococcal polysaccharide. Infect. Immun. **25:**262–267.
26. **McGee, Z. A., and C. M. Clemens.** 1994. Effect of bacterial products on tumor necrosis factor production: quantitation in biological fluids or tissues. Methods Enzymol. **236:**23–31.
27. **Mosmann, T.** 1983. Rapid colorimetric assay for cellular growth and survival: application to proliferation and cytotoxicity assays. J. Immunol. Methods **65:**55–63.
28. **Murphy, J. A.** 1989. Immunoregulation in cryptococcosis. Marcel Dekker, New York, N.Y.
29. **Naslund, P. K., W. C. Miller, and D. L. Granger.** 1995. *Cryptococcus neoformans* fails to induce nitric oxide synthase in primed murine macrophage-like cells. Infect. Immun. **63:**1298–1304.
30. **Platts-Mills, T. A., and K. Ishizaka.** 1974. Activation of the alternate pathway of human complement by rabbit cells. J. Immunol. **113:**348–358.
31. **Stuehr, D. J., and M. A. Marletta.** 1987. Synthesis of nitrite and nitrate in murine macrophage cell lines. Cancer Res. **47:**5590–5594.
32. **Varma, A., and K. J. Kwon-Chung.** 1992. DNA probe for strain typing of *Cryptococcus neoformans*. J. Clin. Microbiol. **30:**2960–2967.
33. **Vecchiarelli, A., D. Pietrella, M. Dottorini, C. Monari, C. Retini, T. Todisco, and F. Bistoni.** 1994. Encapsulation of *Cryptococcus neoformans* regulates fungicidal activity and the antigen presentation process in human alveolar macrophages. Clin. Exp. Immunol. **98:**217–223.
34. **Wilson, M. A., and T. R. Kozel.** 1992. Contribution of antibody in normal human serum to early deposition of C3 onto encapsulated and nonencapsulated *Cryptococcus neoformans*. Infect. Immun. **60:**754–761.
35. **Young, B. J., and T. R. Kozel.** 1993. Effects of strain variation, serotype, and structural modification on kinetics for activation and binding of C3 to *Cryptococcus neoformans*. Infect. Immun. **61:**2966–2972.

Editor: R. E. McCallum